A rheometer for the measurement of a high shear modulus covering more than seven decades of frequency below 50 kHz

T. Christensen and N. B. Olsen
IMFUFA, Roskilde University Center, Postbox 260 DK-4000 Roskilde, Denmark

(Received 28 December 1994; accepted for publication 22 May 1995)

A new rheometer is described. It consists of a transducer unit supplied with an electric impedance analyzing unit. The transducer unit converts a mechanical impedance into an electrical impedance by the piezoelectric effect. A detailed quantitative analysis of the interaction between the sample and the transducer is given. The real and imaginary parts of the shear modulus of a viscoelastic sample can be found in the frequency range of 1 mHz–50 kHz, modulus range of 0.1 MPa–10 GPa, and the temperature range of 150–300 K. The sample volume is 0.3 cm^3 and the strain amplitude is exceedingly small. The small size of the transducer allows for good temperature control and equilibration. It has a simple construction based on inexpensive components. Results on the supercooled liquid 2-metyl-2,4-pentandiol at the glass transition obtained by the method are included. © *1995 American Institute of Physics.*

I. INTRODUCTION

The purpose of this paper is to give a detailed description of a shear modulus rheometer especially suited to the study of liquids with high shear modulus (>1 MPa) in the audio frequency range and below. Since it is based on piezoelectric ceramics we will call it the piezoelectric shear modulus gauge (PSG). It was developed with the aim of studying the frequency dependence of the shear modulus of supercooled liquids at the glass transition. The PSG has been utilized in two recent works. The first dealt with the connection between the electrical and mechanical relaxation in 1,3-butanediol and a silicone oil.[1] The second dealt with the connection between the shear and bulk modulus of 1,2,6-hexantriol.[2] In the latter, a device called the piezoelectric bulk modulus gauge (PBG)[3] was used. It is based on much the same principles as the PSG.

In the case of liquids with a high modulus, one faces physical conditions which make the most common methods fail. Reviews on a variety of such methods have been given by Ferry[4] and Read, Dean, and Duncan.[5]

Following the latter authors one can divide mechanical dynamic methods into four classes:

(1) Forced vibration nonresonance methods (a continuous frequency range below 1 kHz).
(2) Torsional pendulum performing free vibrations (discrete frequencies ranging from 10 mHz to 10 Hz).
(3) Audiofrequency resonance techniques (discrete frequencies ranging from 20 Hz to 20 kHz).
(4) Ultrasonic methods (ranging from 100 kHz to 100 MHz).

The significant parameter is the ratio of the wavelength to a characteristic sample size. This ratio is decreasing down through the list.

The rheometer, PSG, described here uses a forced vibration nonresonance method but is also able to include continuously the frequency range of the resonance techniques. The high frequency limit on the forced vibration nonresonance methods is the first resonance frequency of the apparatus. For the PSG this resonance frequency is moved to a high frequency (~100 kHz) since the mass of the system is much lower than in other rheometers. The demand on rigidity of the rheometer usually sets the dimensions of it and these again imply a certain lower mass limit. The PSG, however, shall not be rigid compared to the sample but must have a stiffness comparable to it. Thus the mass can be considerably lower.

Another distinction between rheometers can be made according to their working principle.[6] They can be based either on (A) a separate driver and sensor, or on (B) only one electromechanical transducer.

In case (A) the driver produces a known strain (or alternatively, a stress) and the sensor registers the resulting stress (or, respectively, a strain). This principle works well in the case of soft materials (e.g., below 1 MPa) but at high moduli not only the sample but also the driver or sensor are strained. Thus one has to take into account the compliance of the apparatus. This can, of course, be done but it is a nuisance which goes against the principle of measuring the pure stress and strain at the sample. Since the rheometer is not fundamentally designed to be strained it becomes difficult to calculate the corrections to be made and thus to make precise measurements.

In case (B) the electromechanical transducer acts as a converter of a mechanical impedance (i.e., the ratio between stress and strain rate) into an electrical impedance. The mechanical impedance of the transducer and the sample should be matched in order to obtain the highest sensitivity. The deformation of the transducer is thus not a problem, but a precondition for this method. Hence the impedance conversion method is the most natural to use in the case of high moduli. An adequate physical and mathematical description of the interaction between the sample and the transducer and of the connection between the mechanical and electrical side of the transducer is, of course, now essential. The transducer must be designed in such a simple way that such calculations are manageable. This can be accomplished by choosing a geometry of such high symmetry that the strain field only depends on one spatial coordinate. The equations of motion

Downloaded 02 Oct 2006 to 130.226.199.12. Redistribution subject to AIP license or copyright, see http://rsi.aip.org/rsi/copyright.jsp

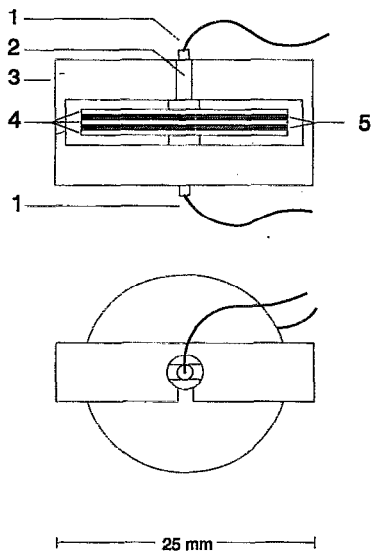

FIG. 1. Side and top view of the piezoelectric shear modulus gauge (PSG). (1) The supply lines for the electrodes. (2) The slit to facilitate assembly. (3) The aluminum casing. (4) The three piezoceramic discs. (5) The two liquid layers.

which are originally partial differential equations will then reduce to ordinary differential equations that are explicitly solvable. In the case of the PSG one has a cylindrical symmetry where the strain field to a good approximation depends on radius only. In the case of the PBG[3] one has a spherical symmetry where the displacement is truly radial.

II. DESCRIPTION OF THE PSG

The device is based on the following simple idea: a piezoceramic material coated with two electrodes acts as an electrical capacitor, the capacity of which is dependent on its strain state. A mechanically clamped capacitor will show a lower value of the capacitance than a free, movable capacitor. If the capacitor is brought into mechanical contact with another material, then this material will clamp the capacitor partially. The resulting decrease in the capacitance will be a measure of the stiffness of the adherent material. The measuring principle is of the impedance conversion type (B).

The realization of this idea actually requires a sandwich structure of three piezoceramic discs (pz discs) with two intermediate layers of liquid (see Fig. 1). The three pz discs are electrically connected as shown in Fig. 2. The middle capacitor is in parallel with the series connection of the two outer capacitors. The three capacitors act as one unit as seen from the outer two terminals. The three discs are oriented with the polar axis in the same direction but the electric field orientation of the middle one is in the opposite direction. On applying a voltage difference to the outer terminals the middle disc will perform a radial displacement and so will the outer discs but in the opposite direction. These displacements produce a strain field in the interlying liquid layers. This is approximately a shear strain field when the liquid layer thickness $3d$ is much smaller than the radius R_0 of the discs.

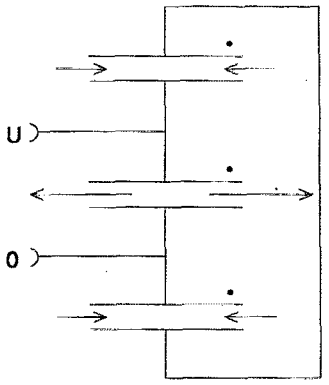

FIG. 2. The electric connection of the three piezoceramic capacitors of Fig. 1. The dots indicate the polarization directions of the piezoceramics. The outer piezoceramic discs move in the opposite direction and only half the distance of the middle disc due to the electric coupling. This holds true even for the liquid filled transducer since the mechanical load of the outer discs are half that of the middle disc.

The construction based on three pz discs is robust, preventing bending motion. A two-disc device consisting of two pz discs moving in opposite directions and with the liquid layer placed in between would give rise to such an unwanted bending.

In the three-disc device the middle disc will experience an external tension twice as big as each of the outer discs. Therefore the three discs are electrically connected to give the middle disc twice the voltage of the outer discs (Fig. 2). The inner tensions produced by the piezoelectrical effect are then also doubled in the middle disc. This ensures that the middle disc always moves twice as far as the outer discs irrespective of the mechanical load of the liquid. Thus, a feature of the liquid displacement field is that it has two neutral planes at fixed distances d (1/3 of the layer thickness) from the outer discs. These neutral planes are vertical to the symmetry axis and there is no radial motion of any point belonging to these planes. They can be regarded as an infinitely rigid support. This means that the mathematical problem of finding the dependence of the electrical capacitance of the device on the shear modulus of the liquid can be mapped onto the problem of a one-disc device (see Fig. 3).

In the one-disc device the liquid is placed between one pz disc and an infinitely rigid support. The one-disc device can be realized (and has been) in the case of liquids of such low shear modulus that it cannot strain the support.

In the three-disc device the pz discs also perform a de-

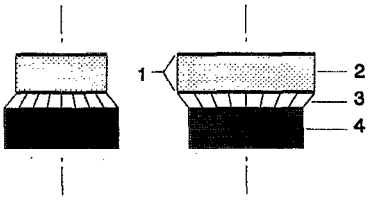

FIG. 3. Schematic presentation of a one-disc device in two extreme positions. (1) The electrodes. 2) The piezoceramic material poled in axial direction. (3) The liquid sample. (4) The infinitely rigid support.

Downloaded 02 Oct 2006 to 130.226.199.12. Redistribution subject to AIP license or copyright, see http://rsi.aip.org/rsi/copyright.jsp

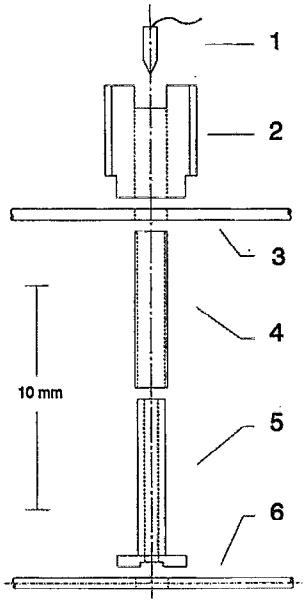

FIG. 4. The central part of the PSG blown apart along the central symmetry axis. The central plane of the PSG vertical to the symmetry axis and bisecting the middle piezoceramic disc is a symmetry plane. Thus only the upper part is shown. (1) The electrode supply line for the electrodes to be plugged into (5). (2) The hollow brass screw to accomplish fixation in the aluminum case (not shown, see Fig. 1). This screw, its twin, and the housing provide the electrical connection between the outer discs. (3) The upper piezoceramic disc. (4) The insulating jacket, preventing connection between (2) and (5). (5) The tubular brass electrode contact and spacer for those two electrodes of the upper and middle pz discs that are facing the upper liquid layer. The assembled device is filled by inserting a syringe into this tube. The slot in the spacer allows the liquid to flow into the spacing between the pz discs. (6) The middle piezoceramic disc.

formation in the polar (z) direction. However the middle and outer discs are also in counterphase in this motion. The thickness of each liquid layer is thus not affected, only a small translational motion is produced. Details of the central part of the three-disc transducer (PSG) have been given in Fig. 4.

Notice that the two electrodes facing one liquid layer are on the same electrical potential and that there is no electric field in the liquid. Such a field would invalidate the method since the liquids under study often have a high dielectric constant and moreover show dielectric relaxation besides the mechanical relaxation.

The small size of the transducer has the benefit of easy placement, thermal control in a cryostat, and avoidance of thermal gradients. In addition, only a small amount of the liquid sample (0.3 cm^3) is needed.

III. THEORY OF THE PSG

A. Basic theory

In the following, a description of how the shear modulus $G(\omega)$ can be deduced from the measured electrical capacitance $C_m(\omega)$ of the PSG will be given. As previously mentioned, the problem is equivalent to that of a one-disc device (Fig. 3). The liquid layer thickness d is 1/3 that of one of the real liquid layers and the capacitance is 3/2 times the individual capacitances of Fig. 2. The radius of the piezoceramic disc is R_0 and the thickness is h.

Place a Cartesian coordinate system with base vectors (e_x, e_y, e_z) at the center of the pz disc, e_z, in the axial direction. The equations are set up in cylinder coordinates (r, ϕ, z). These refer—in the neighborhood of $r = r\cos(\phi)e_x + r\sin(\phi)e_y + ze_z$—to the radial e_r, the azimuthal e_ϕ, and the axial e_z unit vectors. A material point lays at r before the displacement and at r' after the displacement. The displacement field is $u(r) = r' - r = u_r e_r + u_\phi e_\phi + u_z e_z$. The strain tensor becomes[7]

$$\epsilon_{rr} = \frac{\partial u_r}{\partial r}, \quad \epsilon_{\phi\phi} = \frac{1}{r}\frac{\partial u_\phi}{\partial \phi} + \frac{u_r}{r}, \quad \epsilon_{zz} = \frac{\partial u_z}{\partial z},$$

$$\epsilon_{\phi z} = \frac{1}{2}\left(\frac{1}{r}\frac{\partial u_z}{\partial \phi} + \frac{\partial u_\phi}{\partial z}\right), \quad \epsilon_{rz} = \frac{1}{2}\left(\frac{\partial u_r}{\partial z} + \frac{\partial u_z}{\partial r}\right), \tag{1}$$

$$\epsilon_{r\phi} = \frac{1}{2}\left(\frac{\partial u_\phi}{\partial r} - \frac{u_\phi}{r} + \frac{1}{r}\frac{\partial u_r}{\partial \phi}\right).$$

The cylindrical symmetry gives $u_\phi = 0$ and the independence of u_r and u_z on ϕ. Thus, for the two components that will appear to be relevant, one has

$$\epsilon_{rr} = \frac{\partial u_r}{\partial r}, \quad \epsilon_{\phi\phi} = \frac{u_r}{r} \tag{2}$$

while $\epsilon_{\phi z} = \epsilon_{r\phi} = 0$. The last two components, ϵ_{zz} and ϵ_{rz}, are not vanishing but do not enter into the problem as will be seen.

The elastoelectric compliance matrix of a piezoceramic with axial symmetry along the pole axis (z axis) has the same form as that of the crystal class $6mm$.[8] This has the favorable property of a decoupling into four parts, namely

$$\begin{pmatrix} \epsilon_{\phi z} \\ D_\phi \end{pmatrix} = \begin{pmatrix} s_{44} & d_{15} \\ d_{15} & \epsilon_{11}^T \end{pmatrix} \begin{pmatrix} \sigma_{\phi z} \\ E_\phi \end{pmatrix}, \tag{3}$$

$$\begin{pmatrix} \epsilon_{rz} \\ D_r \end{pmatrix} = \begin{pmatrix} s_{44} & d_{15} \\ d_{15} & \epsilon_{11}^T \end{pmatrix} \begin{pmatrix} \sigma_{rz} \\ E_r \end{pmatrix}, \tag{4}$$

$$\epsilon_{r\phi} = 2(s_{11} - s_{12})\sigma_{r\phi}, \tag{5}$$

and

$$\begin{pmatrix} \epsilon_{rr} \\ \epsilon_{\phi\phi} \\ \epsilon_{zz} \\ D_z \end{pmatrix} = \begin{pmatrix} s_{11} & s_{12} & s_{13} & d_{13} \\ s_{12} & s_{11} & s_{13} & d_{13} \\ s_{13} & s_{13} & s_{33} & d_{33} \\ d_{13} & d_{13} & d_{33} & \epsilon_{33}^T \end{pmatrix} \begin{pmatrix} \sigma_{rr} \\ \sigma_{\phi\phi} \\ \sigma_{zz} \\ E_z \end{pmatrix}, \tag{6}$$

where the superscript T on the dielectric constant indicates constant tension. A change among the variables that are considered independent and dependent in formula (6) can thus be made without involving the coefficients of Eqs. (3)–(5). However, a further simplification can be made. The piezoceramic plate is free to move in the z direction, i.e., $\sigma_{zz} = 0$ on the surface $z = h/2$. At frequencies well below the first thickness resonance there will be no gradient, $\partial/\partial z \sigma_{zz} = 0$, i.e., $\sigma_{zz} = 0$ throughout the piezoceramic plate. The ratio of the thickness resonance to the radial resonance frequency is ap-

Downloaded 02 Oct 2006 to 130.226.199.12. Redistribution subject to AIP license or copyright, see http://rsi.aip.org/rsi/copyright.jsp

proximately $R_0/h=20$. Thus the condition holds even at the lowest radial resonances. So we consider only the following relations:

$$\begin{pmatrix} \epsilon_{rr} \\ \epsilon_{\phi\phi} \\ D_z \end{pmatrix} = \begin{pmatrix} s_{11} & s_{12} & d_{13} \\ s_{12} & s_{11} & d_{13} \\ d_{13} & d_{13} & \epsilon_{33}^T \end{pmatrix} \begin{pmatrix} \sigma_{rr} \\ \sigma_{\phi\phi} \\ E_z \end{pmatrix}. \tag{7}$$

If ϵ_{rr}, $\epsilon_{\phi\phi}$, and E_z are chosen as the input variables (independent variables), then

$$\begin{pmatrix} \sigma_{rr} \\ \sigma_{\phi\phi} \\ D_z \end{pmatrix} = \begin{pmatrix} c_{11} & c_{12} & -e_{13} \\ c_{12} & c_{11} & -e_{13} \\ e_{13} & e_{13} & \epsilon_{33}^S \end{pmatrix} \begin{pmatrix} \epsilon_{rr} \\ \epsilon_{\phi\phi} \\ E_z \end{pmatrix}, \tag{8}$$

where the superscript S on the dielectric constant indicates constant strain in the r and ϕ directions and constant tension in the z direction. Denoting Poissons' cross-contraction ratio by $p \equiv -s_{12}/s_{11}$ and the planar coupling factor[8] by

$$k_p \equiv \left(\frac{2d_{13}^2}{\epsilon_{33}^T (s_{11}+s_{12})} \right)^{1/2},$$

one has

$$\begin{aligned} c_{11} &= \frac{1}{s_{11}+ps_{12}}, \quad c_{12} = \frac{p}{s_{11}+ps_{12}}, \\ e_{13} &= \frac{d_{13}}{s_{11}+s_{12}}, \quad \epsilon_{33}^S = \epsilon_{33}^T (1-k_p^2). \end{aligned} \tag{9}$$

Let Q be the charge and U the potential difference of the electrodes of the pz disc. The capacitance $C_m = Q/U$ is the measured quantity. Now $U = E_z t$ and

$$Q = \int_0^{R_0} 2\pi r D_z(r) dr. \tag{10}$$

The free capacitance C_f, defined by $\sigma_{rr} = \sigma_{\phi\phi} = \sigma_{zz} = 0$, becomes

$$C_f = \pi \epsilon_{33}^T \frac{R_0^2}{h} \tag{11}$$

and the clamped capacitance C_{cl}, defined by $\epsilon_{rr} = \epsilon_{\phi\phi} = 0$ and $\sigma_{zz} = 0$ (no vertical clamping), becomes

$$C_{\mathrm{cl}} = \pi \epsilon_{33}^S \frac{R_0^2}{h}. \tag{12}$$

Thus

$$\frac{C_{\mathrm{cl}}}{C_f} = 1 - k_p^2. \tag{13}$$

The coupling factor k_p is a dimensionless measure of the strength of the piezoelectric effect. k_p ranges from zero to one. A value close to one means a strong coupling between the mechanical and electrical ports. Typical values of k_p are 0.1 for quartz, 0.4 for barium titanate ceramic, and 0.6 for lead zirconium titanate ceramic. The piezoceramic type pz26 made by Ferroperm, Denmark and used here is based on the latter material.

From Eqs. (10), (8), and (2) one deduces the measured capacitance,

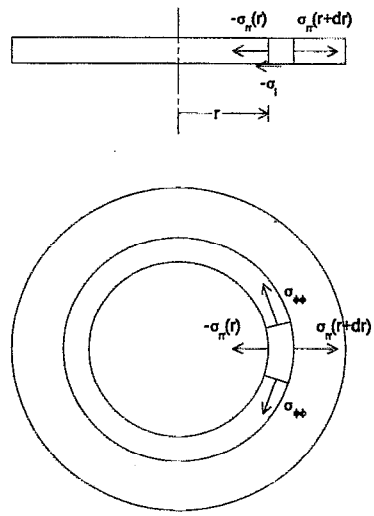

FIG. 5. Illustration of the stresses acting on a differential volume element of the piezoceramic disc.

$$C_m = \frac{2\pi e_{31} R_0}{E_z h} u_r(R_0) + C_{\mathrm{cl}}. \tag{14}$$

Introducing the dimensionless quantity

$$F \equiv \frac{C_m - C_{\mathrm{cl}}}{C_f - C_{\mathrm{cl}}} = \left(\frac{C_m}{C_{\mathrm{cl}}} - 1 \right) \frac{1-k_p^2}{k_p^2}, \tag{15}$$

one finds

$$F = \frac{1}{E_z R_0 d_{31}} u_r(R_0). \tag{16}$$

By Eq. (15) F is directly given by the measurable quantity C_m. It is left to find the displacement $u_r(R_0)$ of the edge of the pz disc as a function of the shear rigidity G of the liquid and to invert this function.

Now consider a differential element of the piezoceramic (Fig. 5). The resulting force per volume transmitted through the surfaces is the divergence of the stress tensor. The expression for this divergence in cylindrical coordinates is given by Sokolnikoff.[9] Making this equal to the density, ρ times the acceleration, one arrives at the radial equation of motion of the piezoceramic plate

$$\frac{1}{r}\frac{\partial}{\partial r}(r\sigma_{rr}) - \frac{1}{r}\sigma_{\phi\phi} + \frac{1}{r}\frac{\partial}{\partial \phi}\sigma_{r\phi} + \frac{\partial}{\partial z}\sigma_{rz} = \rho \frac{\partial^2}{\partial t^2} u_r. \tag{17}$$

The third term is zero since by Eq. (5) $\sigma_{r\phi}$ is proportional to $\epsilon_{r\phi}$, which is zero. The tangential stress σ_{rz} is zero at the free side ($z = h/2$) and $-\sigma_l$ on the side ($z = -h/2$) which is in contact with the liquid. Since the plate is thin ($h \ll R_0$), the gradient $\partial/\partial z \sigma_{rz}$ is approximated with $-\sigma_l/h$. In the following harmonic time variation of E_z and u_r at cyclic frequency, ω is assumed and the factor $e^{-i\omega t}$ is eliminated. E_z and u_r now refer to the amplitude of these fields. Then Eq. (17) becomes

$$\frac{1}{r}\frac{\partial}{\partial r}(r\sigma_{rr}) - \frac{1}{r}\sigma_{\phi\phi} - \frac{1}{h}\sigma_l = -\omega^2 \rho u_r. \tag{18}$$

Downloaded 02 Oct 2006 to 130.226.199.12. Redistribution subject to AIP license or copyright, see http://rsi.aip.org/rsi/copyright.jsp

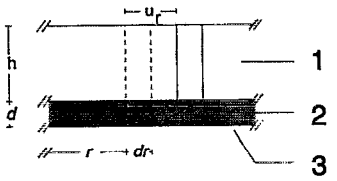

FIG. 6. Illustration of the radial displacement of a differential element of the piezoceramic disc and the shear deformation of the corresponding differential element of the liquid. (1) The piezoceramic disc including electrodes. (2) The liquid layer. (3) The infinitely rigid support.

A further assumption is that the deformation in the liquid is pure shear and that only the component $\epsilon_{rz}^{\text{liquid}}(r)$ is nonzero. This approximation holds because $d \ll R_0$. Then (Fig. 6)

$$\sigma_l = 2G(\omega)\epsilon_{rz}^{\text{liquid}} = G(\omega)\frac{u_r(r)}{d}, \tag{19}$$

where $G(\omega)$ is the shear modulus of the liquid.

Using Eqs. (2), (8), and (19) the tensions of Eq. (18) can be expressed by the displacement u_r,

$$r^2 u_r'' + r u_r' + \left\{ \left(\frac{\omega^2 \rho}{c_{11}} - \frac{G(\omega)}{c_{11} dh} \right) r^2 - 1 \right\} u_r = 0, \tag{20}$$

where differentiation with respect to r now is indicated by an apostrophe. The boundary conditions of this differential equation are zero displacement at the center,

$$u_r(0) = 0 \tag{21}$$

and zero stress at the edge, $\sigma_{rr}(R_0) = 0$ or using Eqs. (8), (9), and (2)

$$u_r'(R_0) + \frac{p}{R_0} u_r(R_0) = (1+p) d_{31} E_z. \tag{22}$$

The problem becomes dimensionless by the following definitions:

$$x \equiv r/R_0, \quad e(x) \equiv \frac{1}{(1+p) d_{13} E_z R_0} u_r(R_0 x). \tag{23}$$

Define the characteristic as follows:

$$\text{modulus} \quad G_c \equiv \frac{c_{11} dh}{R_0^2}, \tag{24}$$

$$\text{inertance} \quad M_c \equiv \rho dh, \tag{25}$$

and

$$\text{frequency} \quad 2\pi f_c \equiv \omega_c \equiv \sqrt{\frac{G_c}{M_c}} = \sqrt{\frac{c_{11}}{\rho R_0^2}}, \tag{26}$$

together with

$$V \equiv \frac{G(\omega)}{G_c}, \quad S \equiv \left(\frac{\omega}{\omega_c} \right)^2, \quad k^2 \equiv S - V. \tag{27}$$

Then Eq. (20) becomes a Bessel differential equation

$$x^2 e'' + x e' + (k^2 x^2 - 1) e = 0 \tag{28}$$

with boundary conditions

$$e(0) = 0, \tag{29}$$

$$e'(1) + p e(1) = 1. \tag{30}$$

The dimensionless measure (16) of the measured electrical capacitance becomes

$$F(\omega) = (1+p) e(1). \tag{31}$$

$e(1)$ is by Eq. (28) a function of k and thereby ω. The solution of Eq. (28) is given by first-order Bessel functions

$$e(x) = A J_1(kx) + B Y_1(kx). \tag{32}$$

Equation (29) yields $B = 0$, while Eq. (30) leads to

$$A = [k J_1(k) + p J_1(k)]^{-1} = [k J_0(k) + (p-1) J_1(k)]^{-1}. \tag{33}$$

Thus the measured electrical capacity C_m becomes

$$C_m(\omega) = C_{\text{cl}} \left\{ F[S(\omega), V(\omega)] \frac{k_p^2}{1 - k_p^2} + 1 \right\}, \tag{34}$$

where

$$F(S,V) = (1+p) \frac{J_1(k)}{k J_0(k) + (p-1) J_1(k)} \tag{35}$$

and

$$k = \sqrt{S - V} = \sqrt{\left(\frac{\omega}{\omega_c} \right)^2 - \frac{G(\omega)}{G_c}}. \tag{36}$$

The resonances occur for those $k = k_n$, $n = 1,2,...$, which satisfy

$$0 = k_n J_0(k_n) + (p-1) J_1(k_n). \tag{37}$$

Thus the resonances depend on Poissons' ratio p. A numerical solution of Eq. (37) gives approximately

$$k_1(p) = 0.621p + 1.861, \quad 0.2 < p < 0.4, \tag{38}$$

$$k_2(p) = 0.192p + 5.332, \quad 0.2 < p < 0.4, \tag{39}$$

and so approximately

$$p(k_2/k_1) = -1.417 k_2/k_1 + 4.032, \tag{40}$$

$$2.5 < k_2/k_1 < 2.75.$$

$f_i \equiv f_c k_i$ are the measured dimensional resonance frequencies of an empty transducer $[G(\omega) = 0]$. Since $f_2/f_1 = k_2/k_1$, Eq. (40) makes it possible to determine Poissons' ratio directly from the observed first and second resonance frequencies without knowing the characteristic frequency f_c. p is found to be 0.31 within a variation of 3% in the temperature interval of 180–250 K. This variation is neglected in the following. Thus

$$k_1 = 2.054, \quad k_2 = 5.391 \quad \text{for } p = 0.31. \tag{41}$$

The zeros of F occur for those $k = j_n$, $n = 1,2,...$, which satisfy

$$0 = J_1(j_n). \tag{42}$$

The first two are $j_1 = 3.8317$ and $j_2 = 7.0156$. Hence it is possible to determine C_{cl} as the measured capacitance at the first antiresonance frequency

Downloaded 02 Oct 2006 to 130.226.199.12. Redistribution subject to AIP license or copyright, see http://rsi.aip.org/rsi/copyright.jsp

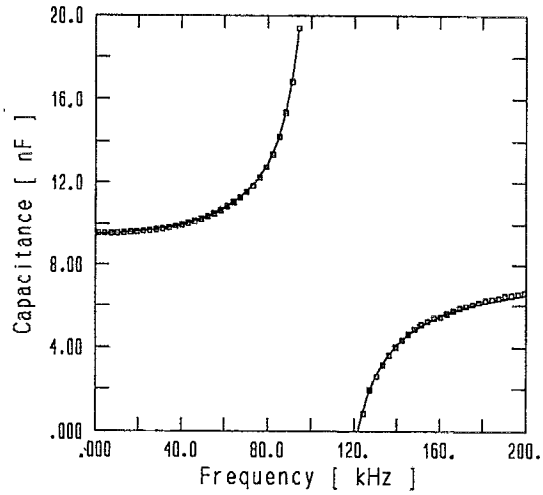

FIG. 7. The first resonance of the empty piezoelectric shear modulus gauge (PSG), at 194 K as seen in the measured real electric capacitance. The symbols □ represents measured data. The fit to the theory (solid line) determines the calibration parameters. These are needed for the inversion of electric capacitance data of the liquid filled PSG into shear modulus.

$$f_{a1}=\frac{j_1}{k_1}f_1=1.865f_1, \quad C_{cl}=C_m(f_a). \tag{43}$$

Figure 7 shows a fit to C_m of the empty transducer at 194 K obtained by suitable scaling. The fitting parameters f_c (or rather $f_1=f_ck_1$) and k_p were varied to give the best possible proportionality between C_m and $Fk_p^2/(1-k_p^2)+1$ at all frequencies. C_{cl} is then given by Eq. (34) as the proportionality constant. At this temperature it was found that $f_1=105.4$ kHz, $k_p=0.56$, and $C_{cl}=6.70$ nF. Typical values of the other characteristic entities can then be given. Since $\rho=7.65\times10^3$ kg m^{-3}, $d=\frac{1}{6}\times10^{-3}$ m, and $h=\frac{1}{2}\times10^{-3}$ m, one has $M_c=\rho dh=6.4\times10^{-4}$ kg m^{-1} and hence $G_c=M_c(2\pi f_1/k_1)^2=6\times10^7$ Pa.

B. Resonance versus quasistatic method

The transducer can, in principle, be used in a very simple way to determine shear modulus G of a substance in temperature ranges, where G shows no dispersion and is real at the resonance frequencies. Denoting $f_i(0)$ and $f_i(G)$ as the ith resonance frequency of the empty and filled transducer, respectively, then according to Eq. (36)

$$k_i^2=\left(\frac{f_i(0)}{f_c}\right)^2=\left(\frac{f_i(G)}{f_c}\right)^2-\frac{G}{G_c} \tag{44}$$

or

$$G=k_i^2G_c\left(\left(\frac{f_i(G)}{f_i(0)}\right)^2-1\right)=(2\pi)^2M_c(f_i^2(G)-f_i^2(0)). \tag{45}$$

Thus G is determined by the movement of the resonances. In practice, however, the thickness and bending (floppy) modes not considered in the present treatment can be problematic for this method.

Indeed, the interest here is in the case of G showing dispersion and the complete solution of Eqs. (34)–(36) has to be used. The determination of G based on the degree of clamping of the electrical capacitance below the first resonance frequency will be termed the quasistatic method.

C. The partially filled transducer

A complication arises when the liquid does not fill out the cell completely. This is inevitable since the cell is filled at $T=300$ K and the measurement is perhaps done at 200 K. With a typical expansion coefficient of 4×10^{-4} K^{-1}, $\Delta R_l/R_l$ becomes 3%. This is of importance since the greatest shear deformation takes place at the edge. Thus an enlarged model with the liquid filling up the cell to radius R_l is considered. Put $x_l=R_l/R_0$. Equation (28) is then replaced by

$$\begin{aligned} &x^2e_1''+xe_1'+[(k_1x)^2-1]e_1=0, \quad k_1^2=\frac{M_c\omega^2-G}{G_c}, \\ &x^2e_2''+xe_2'+[(k_2x)^2-1]e_2=0, \quad k_2^2=\frac{M_c\omega^2}{G_c}. \end{aligned} \tag{46}$$

The boundary conditions are as before plus continuity of displacement and stress at x_l,

$$\begin{aligned} &e_1(0)=0, \quad e_1(x_l)=e_2(x_l), \\ &e_1'(x_l)+\frac{p}{x_l}e_1(x_l)=e_2'(x_l)+\frac{p}{x_l}e_2(x_l), \\ &e_2'(1)+pe_2(1)=1. \end{aligned} \tag{47}$$

Introduce

$$\begin{aligned} &P=k_2J_0(k_2)+(p-1)J_1(k_2), \\ &Q=k_2Y_0(k_2)+(p-1)Y_1(k_2), \\ &R=k_1x_lJ_0(k_1x_l)J_1(k_2x_l)-k_2x_lJ_0(k_2x_l)J_1(k_1x_l), \\ &T=k_1x_lJ_0(k_1x_l)Y_1(k_2x_l)-k_2x_lY_0(k_2x_l)J_1(k_1x_l), \\ &\Delta=PT-RQ, \quad C=T/\Delta, \quad D=-R/\Delta. \end{aligned} \tag{48}$$

Then

$$e_2(1)=CJ_1(k_2)+DY_1(k_2). \tag{49}$$

$e_2(1)$ is by C, D and k_2 a function of V, S, and x_l. F, defined by Eq. (15), now also becomes a function of x_l. It is still given by Eq. (16), such that Eq. (35) is replaced by

$$F(S,V,x_l)=(1+p)e_2(1) \tag{50}$$

while Eqs. (34) and (36) still hold.

D. Inversion algorithm

Before inverting the formulas (34), (50), and (36) to give G as a function of C_m another problem has to be taken into account. C_m is shown again in Fig. 8 but now in a logarithmic plot over a wider frequency span. Below the resonances where C_m is simply equal to C_f a weak dispersion is seen. This reflects dispersion of the dielectric constant $\epsilon_{33}^T\propto C_f$. Similarly, $C_{cl}\propto\epsilon_{33}^S$ will show dispersion, but it is assumed in the following that C_f/C_{cl} and thereby the coupling factor k_p is not frequency dependent. Such a proportionality is not

Downloaded 02 Oct 2006 to 130.226.199.12. Redistribution subject to AIP license or copyright, see http://rsi.aip.org/rsi/copyright.jsp

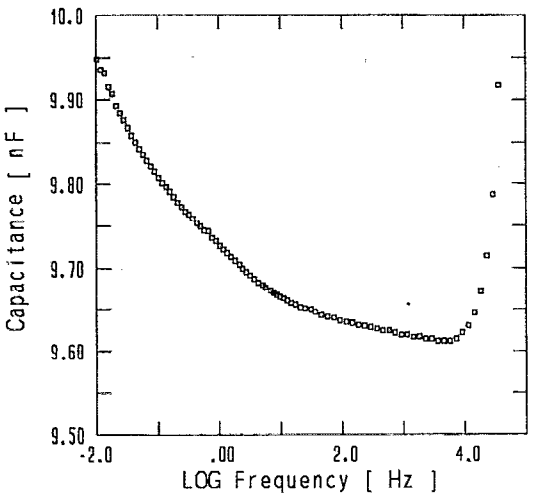

FIG. 8. The real part of the electric capacitance below the first resonance frequency of the PSG at 194 K in a logarithmic frequency scale (log is the base 10 logarithm here and in the following figures). This reveals the weak dispersion of the piezoceramic material itself, an effect which has been taken into account.

found true in general for piezoceramic materials. However this assumption is substantiated in the case of the material pz26 by capacity measurements on partially clamped discs.

Then the frequency dependence can be eliminated in the analysis by considering the ratio of a reference spectrum $C_r(\omega)$ of an empty transducer and a spectrum $C_m(\omega)$ of a filled cell. Introduce

$$\Phi(S,V,x_l)\equiv\frac{C_m-C_{\rm cl}}{C_r-C_{\rm cl}}=\frac{F(S,V,x_l)}{F(S,0,1)}$$
$$=\frac{C_m}{C_r}\left(1+\frac{1-k_p^2}{k_p^2}\frac{1}{F(0,S,1)}\right)$$
$$-\frac{1-k_p^2}{k_p^2}\frac{1}{F(0,S,1)}. \tag{51}$$

$F(S,V,x_l)$, and $F(S,0,1)$, and thus $\Phi(S,V,x_l)$ are known analytically. C_m and C_r can then be measured and thus Φ determined experimentally. All that is left is an inversion to give $V=G(\omega)/G_c$. This is done by approximating Φ with an algebraic expression. Since $\Phi\to 1$ for $V\to 0$ and $\Phi\to 0$ for $V\to\infty$ a broken rational function with the denominator of 1 degree higher than the numerator is chosen

$$\Phi(S,V,x_l)=\frac{1+a(S,\epsilon)V}{1+b(S,\epsilon)V+c(S,\epsilon)V^2}, \tag{52}$$

where $\epsilon=1-x_l$ and

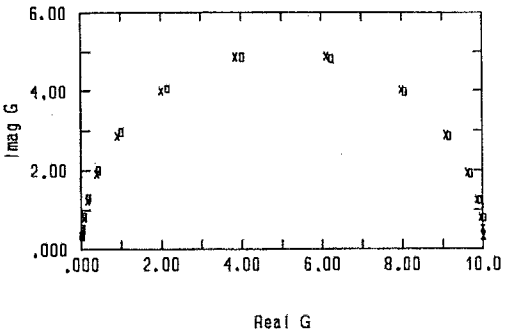

FIG. 9. The approximative algebraic inversion formula checked by applying it to a single relaxation time model of the viscoelastic behavior of a liquid (Maxwell liquid). The elastic modulus G_∞ is a factor of 10 times the characteristic transducer stiffness G_c. The liquid completely fills the transducer. The imaginary and the real parts of the modulus are plotted with the frequency as a parameter (Argand plot). Nearby symbols of the original Maxwell modulus (×) and the calculated modulus (□) are at same frequency.

$$a(s,\epsilon)=\frac{1}{a_1(\epsilon)\left(1-s\,\frac{1}{a_2(\epsilon)}\right)},$$
$$a_1(\epsilon)=25.82(1-0.407\epsilon-22.27\epsilon^2), \tag{53}$$
$$a_2(\epsilon)=13.25(1+0.2\epsilon+11\epsilon^2),$$
$$b(s,\epsilon)=\frac{1}{(4.54+14.7\epsilon)\left(1-\frac{s}{4.22}\right)}, \tag{54}$$
$$c(s,\epsilon)=\frac{1}{(740.+18500.\epsilon)(1-0.287s+0.118s^2)}. \tag{55}$$

This expression approximates Φ within 5% for $0.95<x_l<1.0$ and $0.0<s<4.0$, that is, up to the first resonance of the free transducer.

Inversion of Eq. (52) yields

$$V(S,x_l)=\frac{a-b\Phi+\sqrt{(a-b\Phi)^2-4\Phi c(\Phi-1)}}{2\Phi c}. \tag{56}$$

Figures 9 and 10 illustrate the accuracy of the algebraic fit to

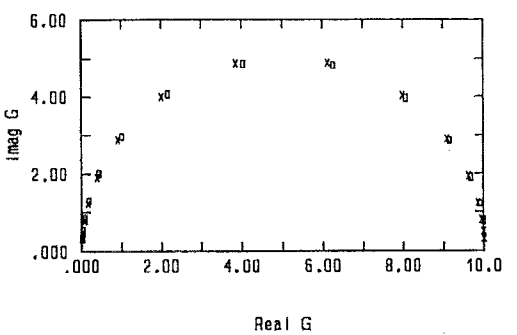

FIG. 10. As in Fig. 9, but now the liquid radius is 95% of transducer radius only.

Downloaded 02 Oct 2006 to 130.226.199.12. Redistribution subject to AIP license or copyright, see http://rsi.aip.org/rsi/copyright.jsp

Φ. These Argand plots show the imaginary versus real part of the modulus of a hypothetical Maxwell liquid

$$G_M(\omega)=G_\infty \frac{-i\omega\tau}{1-i\omega\tau} \tag{57}$$

with $G_\infty/G_c=10$ and a radius $x_l=1.00$ and 0.95, respectively. The crosses are the Maxwell model G_M. The squares are $V(\Phi)$ calculated from Eq. (56) but with Φ calculated from G_M by the analytical formulas (50), (49), (48).

In order to further increase the accuracy in calculating V, one can now resort to a Newton algorithm with the V calculated by Eq. (56) as a trial function V_t. It follows from Eq. (34) that

$$F(S,V,x_l)=\frac{C_m}{C_r}\left[F(S,0,1)+\frac{1-k_P^2}{k_p^2}\right]-\frac{1-k_p^2}{k_p^2}. \tag{58}$$

Denote the value of F calculated by this formula using the measured $C_m(\omega)$ and $C_r(\omega)$ by F_m (the measured F) and the exact V corresponding to this value by V_0. Thus $F_m=F(S,V_0,x_l)$. Since V_0 is near V_t one has

$$F_m-F(V_t)\approx\left(\frac{\partial F}{\partial V}\right)_{V_t}(V_0-V_t)\approx\left(\frac{\Delta F}{\Delta V}\right)_{V_t}(V_0-V_t). \tag{59}$$

This V is complex. A complex derivative is independent of the direction of the differentiation. Let $\Delta V=V_t\delta$, where δ is a small real positive number, that is, differentiate in the direction of V_t. Then

$$F_m-F(V_t)\approx\frac{F[V_t(1+\delta)]-F(V_t)}{V_t\delta}(V_0-V_t) \tag{60}$$

or

$$V_0\approx V_t\left(1+\delta\frac{F_m-F(V_t)}{F[V_t(1+\delta)]-F(V_t)}\right). \tag{61}$$

If one uses the V_0 calculated by Eq. (61) as a new trial function the process can be iterated, since the successive V_t will have V_0 as a fix point. However, Eq. (56) is so close to the exact value that, in practice, one iteration suffices.

IV. APPLICATION

A. Electrical setup

The PSG converts the problem of measuring a mechanical impedance into that of measuring an electrical impedance. The PSG is not tied up with any specific impedance analyzer but the current frequency range and accuracy will depend on it. The PSG and the PBG together with an ordinary capacitor for dielectric measurements make up a series of cheap measuring probes for shear modulus, bulk modulus, and the dielectric constant, respectively. They are applicable for the same impedance analyzer unit and improvements can be made independently.

The Hewlett–Packard HP4192A network analyzer has been used in the frequency range of 10 Hz–50 kHz in measurements on the liquid filled cell. For calibration purposes, the empty cell is measured up to 400 kHz in order to include the first resonance frequency. This was the frequency range covered in the applications[1–3] of the PSG and PBG referred to earlier. The network analyzer was used in the four-terminal impedance mode in those measurements. The HP4192A is now used in the network mode with the oscillator output fed into an external measuring bridge. The PSG impedance is placed in this bridge and the bridge output is connected to a differential amplifier before the detection by the HP4192A. This has substantially decreased the noise at low frequencies and the 5 Hz lower frequency limit of the HP4192A can be exploited. Through supplementation with the Hewlett–Packard multimeter HP3458A, the impedance measurements are now extended into the low frequency range of 10 mHz–100 Hz. In this method another circuit is used. The Keithley Metrabyte digital wave generator PCIP-AWFG supplied with an analog filter feeds a voltage divider consisting of the PSG capacitance and a fixed capacitor of comparable size. The varying voltage over this capacitor is traced by the HP3458A and the amplitude and phase difference are calculated by Fourier analysis in a computer acquiring data. Knowing the network characteristics, the complex PSG capacitance is found. The lower limits of 10 mHz were only set by the limitation of the duration of the experiment. As the impedance rises inversely proportional to frequency, electrical noise becomes more important at low frequency. However, no sign of noise disturbing the method is yet seen at 10 mHz. Thus the low frequency limit could be pushed down one decade or more if necessary. On the other hand, the dispersion of the piezoceramic increases rapidly with decreasing frequency in the case of pz26. Thus probably another material as, e.g., pz29 with a more constant loss should be used in very low frequency studies.

B. Filling

A syringe filled with the liquid sample is introduced from top of the transducer into the central tube (see Fig. 1). This is opened by removing the electrode supply line. In order to fill the transducer in a reasonable time, the temperature is elevated until the viscosity is less than 10^4 Pa s. By application of an adequate pressure, the liquid flows steadily and uniformly through channels in the wall of the central tube and into the spacings between the piezoceramic discs. In order not to produce air bubbles the filling process should be slow enough that wetting of the surfaces can occur. In the case of a transparent liquid such bubbles are easily revealed by simply looking through the liquid from the side of the PSG. The filling is ended when the liquid layer is vertically aligned with the radius of the transducer. The surface tension prevents the liquid from running out.

C. Thermal relaxation of the ceramics

The PSG based on pz26 has been applied successfully in the temperature range of 150–300 K (the ultimate upper limit will be set by the Curie temperature of the piezoceramic). The constitutive parameters are temperature dependent and a calibration is needed at each temperature. However, the structural relaxation occurring in the ceramics when changing the temperature introduces time dependence into these parameters even a long time after thermal equilibrium is reached. This effect is a nonequilibrium effect that is not to

Downloaded 02 Oct 2006 to 130.226.199.12. Redistribution subject to AIP license or copyright, see http://rsi.aip.org/rsi/copyright.jsp

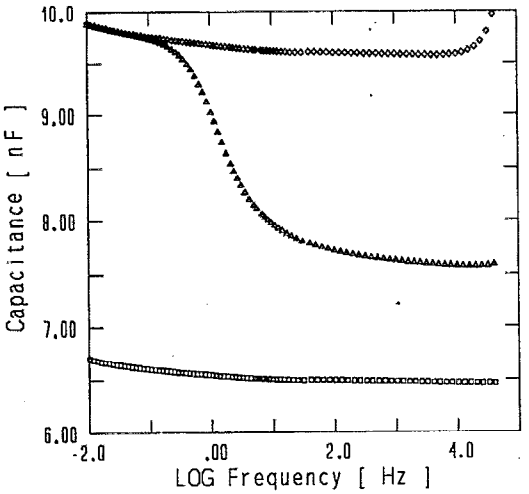

FIG. 11. Electric capacitance measurements at 194 K. The upper curve (◇) is the real part of the capacitance of the empty cell. The lower curve (□) is the calculated capacitance of the clamped cell. The middle curve (△) is the real capacitance of the cell filled with liquid. The decrease of the capacitance with increasing frequency shows the glass transition.

be confused with the equilibrium dispersion discussed in Sec. III D. We have found that reproducible values of the fitting parameters deduced in the resonance calibration procedure can be obtained after repeated heating and cooling, but the relaxation can continue for days. We do not wait for this complete equilibration but wait long enough that the parameters can be considered constant during a measurement. This demands the same time scheme to be followed in the calibration measurement and the liquid measurements. The controlling computer guarantees that the thermal histories are parallel in the two cases. The influence on the final shear modulus results has been examined by repetition of experiments. When the temperature had been shifted, a measurement was made after a waiting time of 45 min. A second measurement was made again after another 45 min. Although the capacitance in the second case had decreased by about 0.5%, the calculated shear modulus based on the two different calibration spectra showed no significant changes.

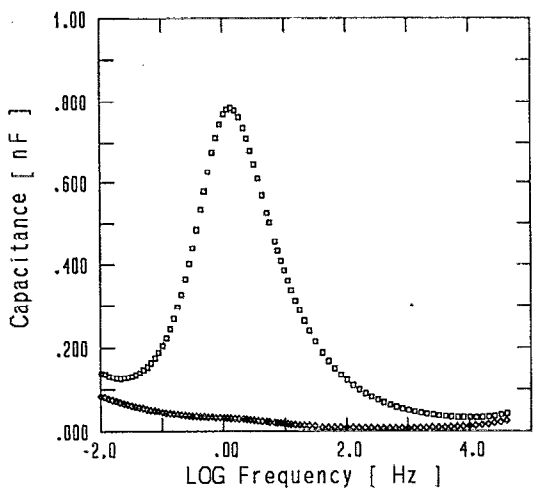

FIG. 12. The imaginary part of the electrical capacitance at 194 K. The lower curve (◇) represents the clamped cell and the upper curve (□) the filled cell.

D. Stress relaxation of the ceramics

When changing the temperature, the liquid placed between the piezoceramic discs tries to contract, thereby creating surface tensions on the piezoceramics. Thus the stress prehistory of the piezoceramic material cannot be the same in the empty and filled transducer. This is of importance at such low temperatures that these biased stresses cannot relax out in the chosen waiting time. The problem, of course, is the worst in the case of liquids with a very high modulus. Fortunately, it is easily detected by considering the reproducibility of the results on first going down and then up in temperature.

E. Measurement

The method has been applied to 2-methyl-2,4-pentanediol, a typical glass former which has been studied in the ultrasonic regime by Meister *et al.*[10] In Fig. 11, data on the directly measured capacitance at 194 K are shown. The upper curve (◇) is the real part of the capacitance of the empty cell, i.e., a reference measurement. As previously mentioned, the coupling factor k_p is found by the fitting of the first resonance peak, and by Eq. (13) the capacity of the clamped cell can be calculated. This is the lower curve (□) of Fig. 11. The middle curve (△) is the real capacitance of the cell filled with liquid. The decrease of the capacitance with increasing frequency shows the glass transition. At low frequencies the liquid curve merges into the curve of the free capacitor. Due to the low modulus of the liquid at these frequencies the PSG is practically free. At high frequencies the liquid curve levels off as the liquid reaches its limiting modulus G_∞. The liquid only partially clamps the transducer and thus any liquid will lie in the window between the free C_f and the clamped C_{cl} values. Correspondingly, the imaginary part of the electrical capacitance is shown in Fig. 12. The conversion of this data into the shear modulus as described in Sec. III is represented in Fig. 13. Both the real and imaginary parts of $G(\omega)$ as a function of the logarithm of frequency are shown. The frequency at which the imaginary part has its maximum is called the loss peak frequency. Notice that although the dispersion region is rather wide it is fully covered by the PSG. The high and low frequency electric impedance measurement techniques join smoothly. As a supplement, an Argand diagram of the imaginary versus the real parts of $G(\omega)$ at 194 K is shown in Fig. 14. The modulus range of 10^5–10^{10} Pa covered by the PSG is illustrated in Fig. 15, where the logarithm of the real and imaginary parts of G versus the logarithm of frequency is shown. The shear modulus of a supercooled liquid is both frequency and temperature dependent, $G=G(\omega,T)$. In Fig. 16 the real part of the shear modulus at a series of temperatures is shown. One sees typically that G_∞ is decreasing with temperature and also that the frequency at which the glass transition sets in is increasing with temperature. In Fig. 17 the logarithm of the

Downloaded 02 Oct 2006 to 130.226.199.12. Redistribution subject to AIP license or copyright, see http://rsi.aip.org/rsi/copyright.jsp

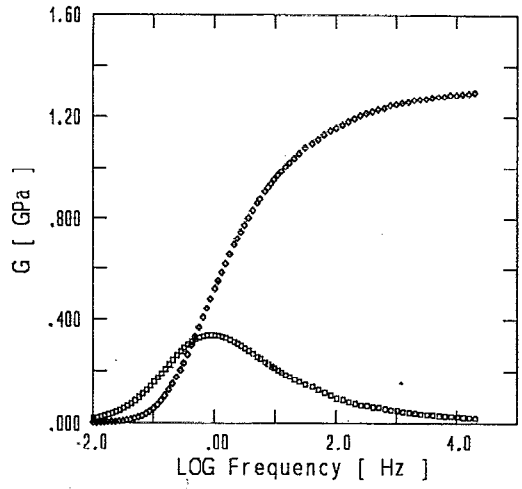

FIG. 13. The real (◇) and imaginary (□) part of $G(\omega)$ as a function of the logarithm of frequency at 190 K. The wide dispersion region of the liquid is fully covered by the PSG. The high and low frequency electric impedance measurement techniques merges at 100 Hz.

loss peak frequencies is shown as a function of temperature in the range where they are covered by the actual frequency window.

The measured values cannot be directly compared to that of Meister *et al.*,[10] since these ultrasonic measurements were done at higher temperatures. Assuming a linear dependence of G_∞ on T, these authors found $G_\infty = 0.294 - 0.0124T$, where G_∞ is expressed in GPa and T in °C. This was based on measurements down to 220 K. An extrapolation of the formula gives 1.35 GPa at 188 K in accordance with the value to be read from Fig. 16. The agreement on the temperature coefficient is, however, not quite as good. Since the uncertainties lie in the absolute rather than the relative determination of G, it is most probable that both methods give a good estimate of $\partial G_\infty/\partial T$ in their respective temperature ranges. This agrees with our findings that this coefficient is decreasing with increasing temperature. The extrapolation should include this nonlinearity in $G_\infty(T)$ and would predict a somewhat higher value of the shear modulus than we have measured.

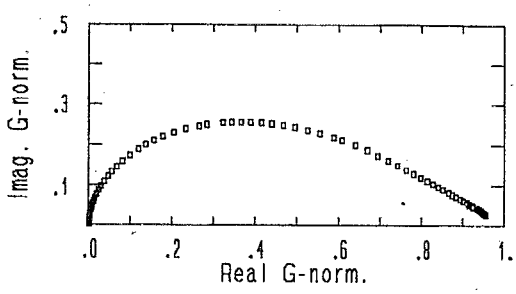

FIG. 14. The Argand diagram of the imaginary vs the real part of $G(\omega)$ at 194 K. The values are normalized by the infinite frequency modulus, 1.25 GPa.

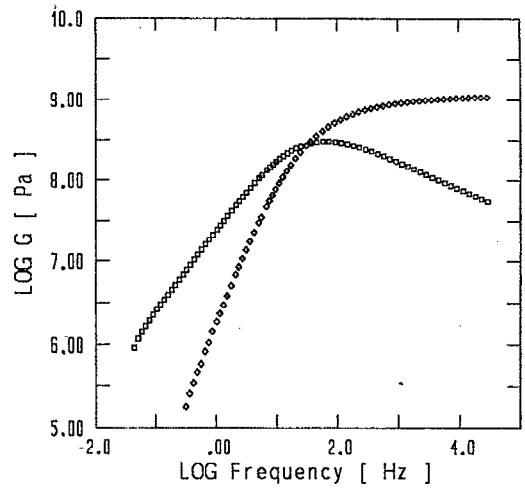

FIG. 15. The most of the modulus range 10^5–10^{10} Pa covered by the PSG is illustrated by showing the logarithm of the real (◇) and imaginary (□) parts of G vs the logarithm of frequency at 198 K.

F. Linearity

The linear laws of viscoelasticity only hold if the strains are not too large. The strains in the case of the PSG are extremely small. The movement of the outer radius of the pz disc is roughly $u_r \approx R_0 d_{13} U/h$, resulting in a liquid shear deformation of $\epsilon_{rz}^{\text{liquid}} \approx d_{13} R_0/hdU$. With $d_{13} \approx 10^{-10}$ C/N and $U = 1$ V, one gets $\epsilon_{rz}^{\text{liquid}} \approx 10^{-6}$, quite a tiny deformation.

V. ACCURACY

A. Sensitivity

The accuracy of the shear modulus measurements depends on the accuracy of the measurement of the electrical capacitance and the sensitivity of the transducer. The sensi-

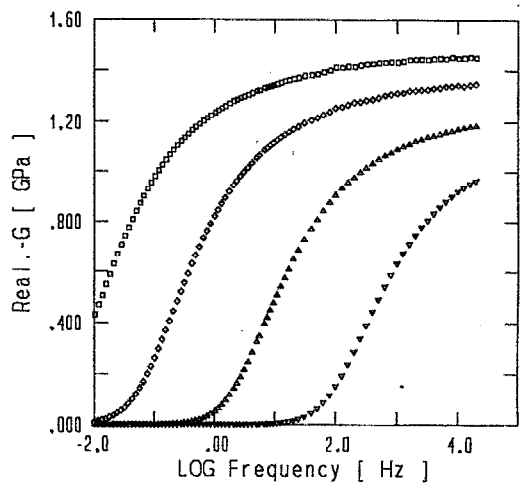

FIG. 16. The real part of the shear modulus at a series of temperatures: (▽) 202 K, (△) 194 K, (◇) 188 K, (□) 184 K. The shift of the curves to lower frequencies as the temperature decreases is a consequence of the increasing internal relaxation time of the liquid.

Downloaded 02 Oct 2006 to 130.226.199.12. Redistribution subject to AIP license or copyright, see http://rsi.aip.org/rsi/copyright.jsp

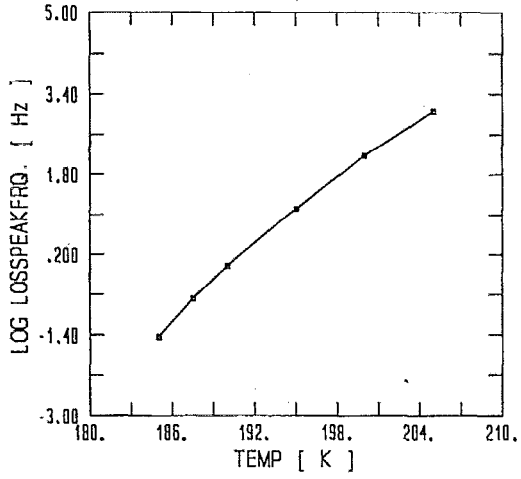

FIG. 17. The logarithm of the loss peak frequencies as a function of temperature in the range where they a covered by the actual frequency window.

tivity Ψ is the ratio between the variation in the normalized measured capacitance F and the relative change in the shear modulus,

$$\Psi = G\frac{\partial F}{\partial G} = \frac{1}{\ln(10)}\frac{\partial F}{\partial \log(G/G_c)}. \tag{62}$$

The sensitivity versus the modulus is shown in Fig. 18 in a logarithmic plot. The PSG is most sensitive at about $5G_c$. At $G=10^6$ Pa one finds $\Psi=0.5\%$. Thus a determination of G within 1% relative accuracy demands an accuracy of 0.005% on the electrical side. This can be achieved by the electrical setup and thus we claim a modulus range of 10^6–10^{10} Pa. Accepting an accuracy of 10%, even 10^5 Pa can be reached. The stated accuracy holds for relative variations. An absolute determination of G is also affected by a number of systematic errors.

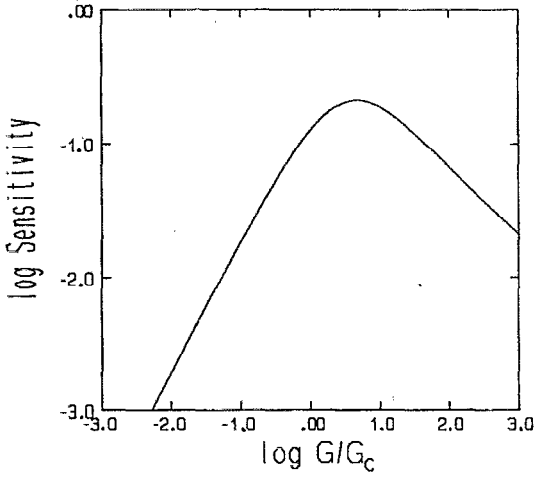

FIG. 18. Transducer sensitivity as a function of the shear modulus of the liquid G relative to the characteristic transducer stiffness G_c. G_c depends on transducer geometry and elastic constants. In our case $G_c=6\times10^7$ Pa.

B. Systematic errors

The largest systematic error comes from the uncertainty of the value of the radius of the liquid layer. An actual radius smaller than assumed will result in a G that is too small. By careful alignment of the liquid and the edge of the PSG, the liquid radius is determined with 0.5%. Using the inversion algorithm, the effect on G is found to be 5%. This is because the inhomogeneous liquid strain field contributes much more to the clamping at the edge than at the center of the piezoceramic plates, and because here the larger differential area per differential radius contributes more to the capacitance. Thus the use of a wrong expansion coefficient of the liquid in the calculation of the radius at lower temperatures will also affect the absolute value of G.

The PSG itself offers a method for estimating the expansion coefficient. At low temperatures, G can be determined not only by the quasistatic method but also by the resonance method (see Sec. III B). The liquid acts as a glassy solid and G has reached its infinite frequency value G_∞. Both methods are dependent on the liquid radius but in a different way and the values only match if the right radius is used.

The part of the liquid layer close to the central axis contributes very little to the overall response. By the same token, the outer part contributes very much. Therefore the partial clamping by the nave can be neglected.

Another systematic error can be ascribed to a volume effect. When the pz disc expands u the relative volume change in the liquid becomes u/R_0, while the shear deformation is u/d. Thus although the deformation is not a pure shear, it is a good approximation in the limit $d/R_0 \ll 1$. In the present case $d/R_0=3\%$. In the theoretical treatment, plate bending has been neglected, although the surface stress $-\sigma_l$ (see Fig. 5) exerted on the pz disc by the liquid has a torque about the azimuthal axis. This is compensated for by torques of radial gradients of σ_{rz} emerging as the disc slightly bends. For reference we notice that the inclusion of this effect involves the constitutive Eq. (4) and the axial equation of motion[9]

$$\frac{1}{r}\frac{\partial}{\partial r}(r\sigma_{rz}) + \frac{1}{r}\frac{\partial}{\partial \phi}\sigma_{\phi z} + \frac{\partial}{\partial z}\sigma_{zz} = \rho\frac{\partial^2}{\partial t^2}u_z. \tag{63}$$

Here the second term on the left-hand side vanishes due to the axial symmetry. Spurious resonances at above 100 kHz can probably be deferred to such floppy modes.

VI. DISCUSSION

A. Some other methods compared

It is not our intention to give a review of other methods—see instead Refs. 4 and 5, but some of the points made in Sec. I can be illustrated by discussing these methods.

Recently, a driver/sensor technique was used by Jeong[11] in the audio frequency range which is a part of the frequency span of the present method. It was applied to glycerol, which has a rather high limiting shear modulus (~4 GPa) compared to other liquids. The driver and sensor were identical X-cut quartz crystals, which—by using the piezoelectric effect—can be given a pure shear deformation when they are free of

Downloaded 02 Oct 2006 to 130.226.199.12. Redistribution subject to AIP license or copyright, see http://rsi.aip.org/rsi/copyright.jsp

surface stresses. These crystals were immersed in the liquid, which again was contained in a copper vessel. It was assumed that the driver determined the strain state of the liquid and that the sensor detects the stress state. Then the relative variations of the shear modulus could be found from the complex ratio of the amplitudes of the output and input voltages for the sensor and driver, respectively. Absolute values were not obtainable.

However, the impact of the liquid on the stress state of the driver or the impact of the sensor on the strain state of the liquid was not taken into account.

The influence of the compliances of the driver and sensor on the output signal will be dependent on the shear modulus of the liquid itself. So this signal can only be assumed to be proportional to G when the stiffness of the liquid is small compared to that of the piezoelectrical crystals. The evaluation of the ratio between the stiffness of the liquid and that of the crystals is difficult without knowing the exact strain field. The stiffnesses involve both the specific moduli and a geometric form factor.[12] The dimensions of the liquid and the crystals are comparable. The deformation of the crystals could involve the smallest modulus $c_{12}=7$ GPa,[13] which is only twice as much as glycerol. If this is the case, the effect can hardly be neglected.

Another problem is that both shear and bulk moduli have to be taken into account since they are of comparable size. Even if the transducers themselves only perform shear deformations preserving the total volume, the volume need not be preserved locally in the liquid. The presence of two independent elastic constants of an isotropic medium implies that one cannot use proportionality arguments and circumvent a calculation of the actual strain field. Such a calculation will, in practice, be impossible due to the complicated boundary conditions induced by the geometry. The rather involved calculations of the even more highly symmetric PSG exemplify this.

The impressive shear modulus apparatus of Ferry and Fitzgerald[14] was based on a conversion of the mechanical impedance into an electrical impedance like the PSG. The transduction was based on electromagnetic instead of piezoelectric effects. The rigidity range was much the same as for the PSG (displaced 1 decade down). This wide range was partly achieved by adjusting the sample impedance using samples of different geometries. This corresponds to changing the characteristic modulus G_c of formula (24), but the sensitivity discussed in Sec. V A was based on one sample geometry only. The frequency range of the Ferry/Fitzgerald apparatus was 25–5000 Hz. The moving part of the transducer had a resonance below 25 Hz that just started to appear at the lower end of the frequency range. This resonance could provide problems in using the apparatus at lower frequencies. The large size of the device was a drawback. It had a weight of 100 kg and a linear dimension of 40 cm. A special cryostat was built for it and thermal equilibrium was established only after a long time. In this respect, the PSG weighing 12 g and having a diameter of 2 cm offers clear advantages.

B. Advantages and disadvantages of the PSG

The special, symmetrical three-plate arrangement of the piezoceramic discs of the PSG has several advantages. First, it stabilizes the mechanical displacement. Second, in combination with the special electric wiring of the three plates, it is possible to analyze the mechanical interaction of the liquid and the transducer in terms of a simple artificial one-device transducer. Extensive calculations on this model have been given, including the effect of partial filling. The necessary calibration parameters besides mass and linear dimensions can be determined by a resonance measurement on the empty transducer. The frequency dependent shear modulus of a liquid filled into the PSG can then be derived from a measurement of the resultant electric capacitance of the transducer. Since high precision electric impedance measurements are readily made, the shear modulus can be determined even when the sensitivity of the device is low. This gives the wide dynamic range (10^5–10^{10} Pa). This range can be expanded by changing the characteristic transducer stiffness, which depends on the geometry. The upper limit of the frequency range is around half the first resonance frequency, i.e., in the present case 50 kHz. The resonance frequency is inversely proportional to the diameter. The lower limit is beyond 1 mHz, which in most work is also a practical limit when it comes to the duration of an experiment. The wide frequency range is of importance in a study of the so-called temperature time scaling principle (TTSP), which some of the relaxation mechanisms at the glass transition seem to follow. Methods with a narrow frequency range can only determine the relaxation function by assuming that this principle be obeyed. The results of Meister *et al.*[10] were obtained in this way. With its wide frequency range, the PSG gives a unique possibility to examine the principle itself. The temperature range is for the time being 150–300 K.

The PSG has a simple construction consisting of a few inexpensive components. The transducer could therefore be considered as a disposable unit in certain destructive experiments as, e.g., hardening studies of glues. The small amount of the sample needed is another benefit of the method, especially in cases where the sample is expensive or difficult to synthesize. The small amount of volume is easy to thermostat because of the short thermal equilibrium relaxation time and thermal gradients are more easily avoided.

The main problems of the method should also be mentioned. The existence of the dispersion and thermal relaxation of the piezoceramic material requires reference spectra at each temperature and a strict parallel thermal history of these and their corresponding liquid spectra. The characteristic flow time needed in the process of thermal contraction of the liquid following a temperature shift increases when the temperature is lowered. Thus at low temperatures and for very high sample shear modulus stress dependent relaxation of the piezoceramic constitutive parameters adds to these complications. The remedy for this is a prolonged annealing time. Although relative variations in shear modulus can be determined with high accuracy (dependent on the position on the sensitivity curve) the absolute value is only determined within 5%. The uncertainty comes mainly from the determination of the radius of the liquid layers.

Downloaded 02 Oct 2006 to 130.226.199.12. Redistribution subject to AIP license or copyright, see http://rsi.aip.org/rsi/copyright.jsp

ACKNOWLEDGMENTS

We would like to thank electrical engineer Ib Høst Pedersen and technician Torben Rasmussen for technical support and Jeppe Dyre for comments on the theory of the PSG.

[1] T. Christensen and N. B. Olsen, J. Non-Cryst. Solids **172**, 357 (1994).
[2] T. Christensen and N. B. Olsen, J. Non-Cryst. Sol. **172**, 362 (1994).
[3] T. Christensen and N. B. Olsen, Phys. Rev. B **49**, 15396 (1994).
[4] J. D. Ferry, *Viscoelastic Properties of Polymers*, 3rd ed. (Wiley, New York, 1980).
[5] B. E. Read, G. D. Dean, and J. C. Duncan, in *Physical Methods of Chemistry*, 2nd ed., edited by B. W. Rossiter and R. C. Baetzold (Wiley, New York, 1991), Vol. VII, p. 1.
[6] Reference 4, p. 114.
[7] L. D. Landau and E. M. Lifshitz, *Theory of Elasticity* (Pergamon, New York, 1970).
[8] B. Jaffe, W. Cook, and H. Jaffe, *Piezoelectric Ceramics* (Academic, New York, 1971).
[9] I. S. Sokolnikoff, *Mathematical Theory of Elasticity*, 2nd ed. (McGraw Hill, New York, 1956).
[10] R. Meister, C. J. Marhoeffer, R. Sciamanda, L. Cotter, and T. Litovitz, J. Appl. Phys. **31**, 854 (1960).
[11] Y. H. Yeong, Phys. Rev. A **36**, 766 (1987).
[12] Reference 4, p. 97.
[13] J. C. Brice, Rev. Mod. Phys. **57**, 105 (1985).
[14] E. R. Fitzgerald and J. D. Ferry, J. Colloid. Sci. **8**, 1 (1953).

Downloaded 02 Oct 2006 to 130.226.199.12. Redistribution subject to AIP license or copyright, see http://rsi.aip.org/rsi/copyright.jsp